separations

MDPI

Article

An Experimental Investigation of the Influence of High-Frequency Standing Sound Waves on Depth Filtration Using Coarse-Pored Media

Jonas Hasenkrug and Rouven Schweitzer *

Machining Technology for Lightweight Materials, Department for Lightweight Construction Technologies, Fraunhofer Institute for Manufacturing Engineering and Automation IPA, Nobelstraße 12, 70569 Stuttgart, Germany; jonas.hasenkrug@ipa.fraunhofer.de

* Correspondence: rouven.schweitzer@ipa.fraunhofer.de

Abstract: When a suspension passes through a high-frequency standing sound wave, the particles it contains are manipulated by acoustic forces. In a one-dimensional sound field, these forces lead to a planar arrangement of the particles and the formation of agglomerates. It is known that the combination of these forces and depth filtration can be utilized to significantly increase the filter efficiency of coarse-pored media. So far, this concept has only been used in microfluidics. In this paper, we present the results of a scaled-up filtration channel to test the viability of the industrial application of acoustically assisted filtration systems for the removal of microparticles. The influences of acoustic power input, flow rate, and the porosity of the filter media are investigated. In addition to verifying the scalability, a significant decrease in the large particle fraction in the outflow of the channel was observed when a high-power sound field is applied. Furthermore, the formed agglomerates tend to rise to the fluid surface. The floating particles mostly consist of a large particle fraction.

Keywords: ultrasonics; filtration; porous media; acoustic radiation force; microplastics

Citation: Hasenkrug, J.; Schweitzer, R. An Experimental Investigation of the Influence of High-Frequency Standing Sound Waves on Depth Filtration Using Coarse-Pored Media. *Separations* **2023**, *10*, 512. https://doi.org/10.3390/separations10090512

Academic Editor: Ki Hyun Kim

Received: 23 August 2023
Revised: 11 September 2023
Accepted: 13 September 2023
Published: 16 September 2023

1. Introduction

The removal of particulate contaminations from liquids has gained an increase in attention in recent years due to the prevalent problem of microplastics [1]. Microplastics classifies plastic particles with a diameter of less than 5 mm [2]. Besides their negative impact on the environment, especially aquatic wildlife [3], industrial processes can also be negatively affected by particulate contaminations. In the machining sector, especially in contract manufacturing, manufacturers work with a mix of materials, ranging from steel, brass and aluminum to carbon fiber reinforced plastics and pure plastics, which are often machined on the same tool machine. This leads to a contamination of the cutting fluid with plastic particles in the form of chips in various sizes. Especially in the case of carbon fiber reinforced plastics, micro-sized highly abrasive fibers can be introduced into the cutting fluid circuit, which can damage pumps, fluid lines, nozzles, linear bearings and other machine parts they come in contact with. Many standard band filter media for machining are not suitable for separating the fiber fragments from the cutting fluid [4]. While a smaller pore size of the filter media can solve this problem, the necessary pressure differential typically leads to high energy consumption by such systems [5]. A different approach is to utilize external fields to manipulate particles [6]. This can be used improve filter efficiency of regular filters by altering particle trajectory, trapping them in gradient fields, increasing the probability of capture or by influencing attractive forces between fiber–particle and particle–particle.

One example of this is magnetic separation, commonly used in machining to remove metal chips from the cutting fluid, where the use of a filter medium becomes obsolete. Since this mechanism cannot be applied to polymers due to their lack of interaction with

magnetic fields, different physical properties must be considered. While differences in density between particles and fluid can usually be used to cause sedimentation or flotation, the differences in density between polymers and water are to small to overcome stabilizing mechanisms such as electrostatic and steric forces. Only when the forces are comparatively high, such as in a centrifuge, separation based on density can be achieved. Another method of separation based on density is the use of highly localized gradients in pressure that can form in high frequency acoustic standing waves.

By utilizing acoustic forces, particles suspended in a liquid medium can be manipulated [7]. When using a high-frequency standing acoustic wave, the local oscillation in pressure leads to a partial segregation of the suspension. This can be attributed to the primary and secondary acoustic forces (PAF and SAF). The primary acoustic force

$$F_{pr.ac} = V_p k E_{ac} \left[\frac{5\Lambda - 2}{2\Lambda - 1} - \frac{1}{\sigma^2 \Lambda} \right] \sin(2kx) \tag{1}$$

causes the solid phase to be pushed into the nodes or antinodes of the standing wave [8], depending on the density ratio $\Lambda = \rho_{particle}/\rho_{liquid}$, the sound velocity ratio $\sigma = c_{particle}/c_{liquid}$, particle volume V_p, acoustic energy density E_{ac}, wave number k, and the distance of the particle relative to the nearest node x. The secondary acoustic force

$$F_{se.ac} = \frac{k^2 E_{ac}}{2\pi} \left[1 - \frac{\gamma_1}{\gamma_f} \right] \left[1 - \frac{\gamma_2}{\gamma_f} \right] \frac{V_1 V_2}{d^2} \tag{2}$$

results from the sound waves being scattered by the solid phase particles and neighboring particles interacting with the scattered sound field, inducing attractive forces between particles in the suspension [9]. The value of $F_{se.ac}$ depends on the compressabilities of the interacting particles $\gamma_{1/2}$ and the fluid γ_f, the volumes of the particles $V_{1/2}$ and their relative distance d.

The combination of both forces causes the particles to be first pushed into the wave nodes or antinodes by the PAF and then to agglomerate through the SAF. The influence of these forces on filtration using coarse porous media was first investigated by Gupta and Feke [10]. They were able to show that the filtration efficiency can be significantly increased by applying standing acoustic waves perpendicular to the direction of flow. They explain the increase in filter efficiency by three possible mechanisms: (I) due to the PAF the particles are driven towards the node or antinode plane and can thereby not pass the filter medium freely, (II) the agglomerates of particles caused by the SAF are more easily retained by the filter medium due to the increase in size and are held in the filter medium due to the PAF, and (III) the SAF can act between particles and elements of the filter medium, attracting particles and improving their adherence.

By using the sound field, filter media can be used which are normally too coarse-pored for filtration. The deactivation of the acoustic fields allows for a large portion of trapped particles to be released from the filter. At a later stage, Gupta and Feke developed a model to describe the trajectory of the particles through the filter medium [11], which was verified by Grossner et al. [12]. A practical application for the filtration concept was found by Wang et al. [13]. They were able to retain mammalian cells in a filter medium with pores that are two orders of magnitude larger than the used cells. However, throughput is a limiting factor for many devices, as they are designed for microfluidic applications. The acoustic channels and sound fields studied so far have mainly been focused on microfluidics. Sample flow rates are typically $<$100 mL min^{-1}, which is insufficient for many industrial applications. As an example, Ostasevicius et al. used a cylindrical standing wave separator with a sample flow rate of roughly 33 mL min^{-1} which is considered twice the rate of microchannel separation [14], while the high-throughput microfluidic systems proposed by Gui et al. can operate at a sample flow rate of 50 mL min^{-1} [15].

Since acoustically assisted filtration shows great potential for the filtration of small particles such as microplastics, its application on a larger scale is of interest. For this reason,

the present work focuses on investigating the scalability the filtration concept in order to test its applicability in industrial processes with higher throughput. Therefore, a larger filtration chamber with higher throughput >100 mL min^{-1} and a more powerful acoustic transducer was built, and is being used for the experimental investigation.

2. Materials and Methods

2.1. Acoustic Filtration Chamber

The experimental setup is schematically shown in Figure 1, and consists of a reservoir with suspension above the inlet, and with a flow measurement to ensure constant flow during the experiment. From there, the liquid enters the custom-made acoustic filtration chamber, shown in Figure 2. In its center portion, the acoustic transducer Sonoplate High Frequency from Weber Ultrasonics with the dimensions 185 mm × 244 mm is installed vertically on the backside of the chamber. Through direct contact with the suspension, its oscillation in the direction perpendicular to its mounting plane introduces a high frequency longitudinal acoustic wave into the liquid. A glass window on the other side of the chamber in front of the transducer acts as the acoustic reflector, while enabling visual observation during the experiments. The distance between transducer and reflector can be adjusted by 4 screws positioned on the back of the chamber, so the distance corresponds to an integer multiple of half the wavelength λ. The travel of the positioning mechanism allows the distance to be set in a range between 10 mm and 140 mm. They also act as a means to ensure parallelism after the distance is set. The multiple inlets and outlets on the sides of the channel are arranged in 3 rows of hose connectors, allowing the experimenter to make the channel more narrow, disconnecting all the unused inlets and outlets. The acoustic field emitted from the transducers surface is limited to an area of 122 mm × 168 mm and it oscillates with a frequency of 1 MHz, which is created by the SonoPower 3S Megasonic Boost ultrasound generator from Weber Ultrasonics. The generator allows for an adjustment of the power output ranging from 0% to 100%, where 100% corresponds to a power input of 500 W. For the experiments, the distance between transducer and reflector was set to 20 mm.

2.2. Particle Suspension

The particle suspension consists of polyamid 12 (PA) particles used for additive manufacturing with a particle size distribution centered around 56 µm. The particles are suspended in a mixture of 97.5 wt% water and 2.5 wt% of the synthetic metalworking fluid Syntilo MR 81 BF produced by Castrol, acting as a surfactant for the particles. 0.5 g/L of PA particles were then added to the solution which resulted in a suspension that remained metastable for a duration of over 24 h, therefore effects of naturally occurring sedimentation and flotation in the course of the experiments can be neglected.

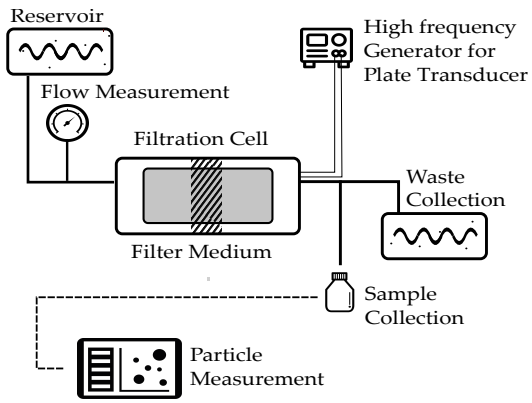

Figure 1. Schematic of the experimental setup.

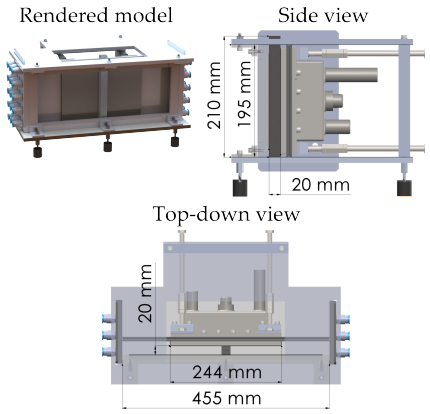

Figure 2. Top-down view of the filtration cell.

2.3. Filter Media

As filter media for the depth filtration, foams made of polyester were purchased from HIRI—Hildebrand und Richter & Co. (Kirchgellersen, Germany) with a porosity of 15, 20 and 30 pores per inch (ppi), with a average pore diameters of 2.54 mm, 1.27 mm and 0.85 mm, respectively. Thus, the pores are at least one magnitude larger than the particles in the suspension. The foams were cut to shape to fit inside the acoustic channel. The filter media have a width of 20 mm, equal to the channel width, and reached from the bottom of the channel up to 15 mm above the liquid surface, so none of the suspension could seep over the filter. A filter depth of 20 mm was chosen, as it is sufficiently deep and only fills a small portion of the acoustic field, so non-filter-related acoustic effects before and after the filter medium could be observed as well. The filter strips were placed vertically in the center of the acoustic channel.

2.4. Methodology

Since no previous experiments on an acoustic depth filtration test setups of comparable size are known to the authors, a design-of-experiments (DoE) approach was chosen. Flow rate Q, acoustic power input P and the porosity Φ were chosen as parameters, and their influence on filtration efficiency was investigated. The values of P serve as a reference value for the acoustic energy E_{ac} contained in the standing wave.

For the flowrate Q values of 0.4 L min^{-1} and 0.8 L min^{-1} were chosen, as they cover a range in which the volume flow is large enough for a reasonable industrial application, but no turbulent flow occurs. P was varied on the levels 0%, 10% and 30%. $P = 30\%$ was chosen as the upper limit because above this threshold, acoustic streaming was observed for the setup present. As for Φ, the aforementioned polyester foams with 15 ppi, 20 ppi and 30 ppi were used, bringing the total amount of configurations tested to 18.

For each configuration, the flow was initially set to the designated value and a sample of 50 mL was drawn from the effluent via a valve in the tubing for a baseline measurement of particle concentration in the suspension. Then, the filter medium was placed in the chamber and the high-frequency generator was activated. From this point on, every two minutes, a sample was drawn from the effluent for a total of 20 min, resulting in 11 samples for each configuration.

2.5. Sample Analysis

The samples were then diluted with demineralized water by a factor of 5 before being analyzed with the flow cell particle counter FC 200M by OCCHIO. Dilution was necessary because the device requires a minimum quantity of 200 mL, and to reduce overlapping of particles in the measurement cell during a measurement. The device pumps a small quantity of liquid from a reservoir into a cuvette, where the liquid within the narrow space is backlit and then photographed. This process is repeated 42 times, and the images taken are then analyzed by the software CALLISTO provided by OCCHIO, where a pixel-based

particle analysis is performed. For each image, the number of particles detected, and their equivalent size and shape are saved in a report file. Each measurement was performed three times, and high reproducibility between measurements was observed. The fluid in the reservoir was stirred to counteract sedimentation or flotation that could result from possible destabilization of the suspension caused by dilution.

With a calibration performed in advance, the concentration C in g/L can be calculated from the number and size distribution of the particles for each sample. The filter efficiency η is then calculated from the ratio of the particle concentration of the initial sample C_0 and the samples in the course of the experiment $C_e(t_i)$ with

$$\eta(t_i) = \frac{C_0 - C_e(t_i)}{C_0}. \tag{3}$$

To describe the portion of particle mass that has been retained by the filter up to a certain time t_i, the retentive filter efficiency η_{ret} is employed, given as

$$\eta_{ret}(t_i) = \frac{1}{i} \sum_{k=0}^{i} \eta(t_k). \tag{4}$$

Since the samples in the outflow are taken at regular intervals, and the flow rate is kept at a constant level, $\eta_{ret}(t_i)$ is equal to the average of the η values measured up to that time.

3. Results

3.1. Visual Observations

In the experimental setup, the filter medium is positioned in front of the center region of the acoustic transducer. Therefore, the particles pass through the sound field and are effected by the acoustic forces before coming in contact with the filter medium. This means that the particles can already be manipulated in advance by the PAF and SAF and agglomerate (see Figure 3). Without the influence of the sound field, no agglomerates were observed. A large portion of the agglomerates that form are larger than the pores of all the filter media considered, which means they can deposit on the filter surface. This converts the filter media, which were originally used as depth filters, into surface filters.

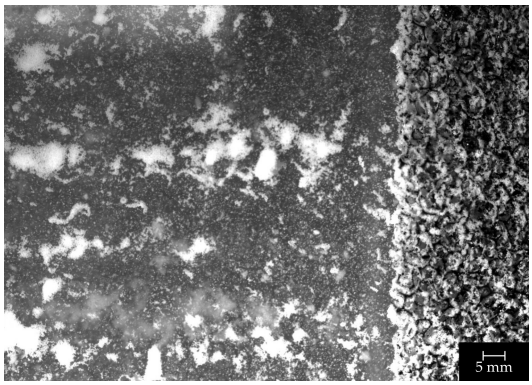

Figure 3. Formation of agglomerates in front of the filter medium (whir); flow direction from left to right, 15 ppi.

The agglomerates that form are more prone to flotation and separate from the suspension at the liquids surface. The measured filter efficiencies therefore do not describe the efficiency of the filter medium, but rather the filter efficiency of the entire experimental setup, including particle separation due to flotation.

3.2. Development of the Filter Efficiencies over Time

To illustrate the temporal evolution of η and η_{ret}, three exemplary progressions with varying frequency generator powers P are shown in Figure 4. The graph of η in Figure 4a

shows a large increase in filter efficiency when a sound field is present. Already at 2 min, when the first sample is drawn, a much lower amount of particles was measured. The evolution of η_{ret} can take one of three forms for the experiments: (I) the retentive filter efficiency constantly increases up until the end of the experiment at 20 min; (II) after reaching its maximum, it stays on a constant level; or (III) after reaching a local maximum, it decreases slowly over time. In Figure 4b, case (I) takes place for $P = 30\%$, case (II) can be observed for $P = 0\%$, and a light version of case (III) can be seen for $P = 10\%$.

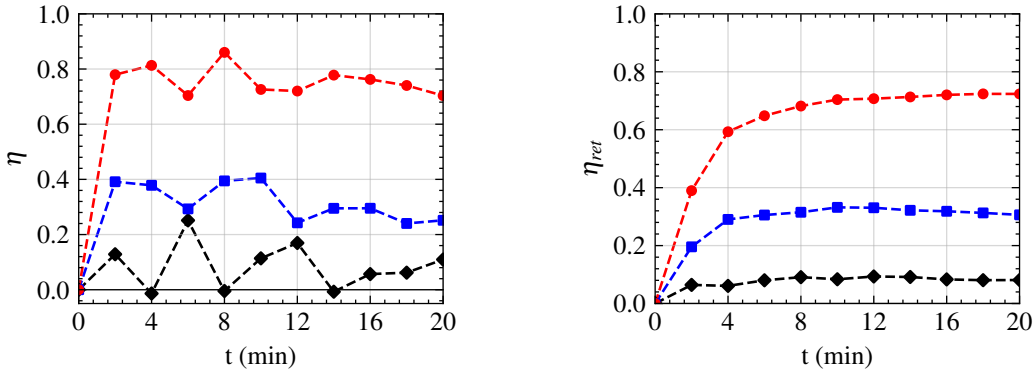

(**a**) Development of η (**b**) Development of η_{ret}

Figure 4. Exemplary temporal developments of the filter efficiencies η and η_{ret} for a porosity of 20 ppi, $Q = 0.8\,\mathrm{L\,min^{-1}}$ and P of 0% (◆), 10% (■) and 30% (●).

3.3. Final Retentive Filter Efficiency

In order to qualitatively compare the filter efficiencies of different test series, the final retentive filter efficiency $\eta_{ret.fin}$ is defined as the retentive filter efficiency η_{ret} that is observed after 20 min. The values of $\eta_{ret.fin}$ for all configurations can be found in Table 1. An analysis of variance (ANOVA) was performed on the results. With α set at 0.05, P and Q were identified as significant influences, with an increase in P leading to an increase in filter efficiency, while lower flow rates Q were also identified as beneficial. The variation in porosity Φ in the selected range had no significant effect.

Table 1. Overview of all values of $\eta_{ret.fin}$.

Q	**0.4 L min^{-1}**			**0.8 L min^{-1}**		
Φ	**15 ppi**	**20 ppi**	**30 ppi**	**15 ppi**	**20 ppi**	**30 ppi**
$P = 30\%$	0.91	0.78	0.75	0.76	0.72	0.64
$P = 10\%$	0.83	0.52	0.46	0.19	0.31	0.31
$P = 0\%$	0.14	0.35	0.28	0.14	0.08	0.23

3.4. Temporal Development of the Retentive Filter Efficiency

As described in Section 3.2, some temporal developments of η_{ret} show a stagnant behavior, while others slowly decline after reaching a maximum or increase until the end. In order to describe this effect, the quantity δ_{10} is introduced, which corresponds to the percentage difference of η_{ret} after 10 min and 20 min. Negative values of δ_{10} reflect a drop of η_{ret} in the last 10 min, values close to 0% represent stagnation, and positive values indicate that the filter can effectively separate particles until the end of the measurement. All values of δ_{10} are presented in Table 2.

With an increase in P, δ_{10} tends to increase and take on mostly positive values. For the flow rate of $0.8\,\mathrm{L\,min^{-1}}$, δ_{10} takes smaller values than the corresponding measurements for $0.4\,\mathrm{L\,min^{-1}}$. A conducted ANOVA shows that the influences of P and Q are indeed significant, while an influence of the Φ can not be derived.

Table 2. Overview of all values of δ_{10}.

Q	**0.4 L min^{-1}**			**0.8 L min^{-1}**		
Φ	**15 ppi**	**20 ppi**	**30 ppi**	**15 ppi**	**20 ppi**	**30 ppi**
P = 30%	+5.8%	+8.8%	+6.3%	+3.0%	+2.0%	−0.1%
P = 10%	+5.7%	−3.1%	+2.4%	−2.1%	−2.6%	−6.3%
P = 0%	+1.4%	−2.1%	−5.3%	+1.2%	−0.3%	−7.6%

3.5. Change in PSD

Since the measurement method used not only measures the particle concentration, but also the particle size distribution, the influence of the parameters investigated on PSD can also be examined.

It can be observed that the PSD in the effluent changes under the influence of the sound field. Thereby, the proportion of particles with a diameter of more than 30 µm decreases significantly compared to the input suspension. This significant change in the PSD does not occur in the tests without the sound field. For a better understanding, three PSDs of an experiment with $P = 30\%$ are visualized in Figure 5. While the input suspension shows particles with diameters under and above 30 µm, the effluent suspension shows nearly no particles with a diameter above 30 µm. In addition, a sample of the particle that collected on the fluids surface was taken, where rising agglomerates were floating on top. The sample was diluted and stirred, so that the agglomerates broke down into single, detectable particles. Their PSD in Figure 5c shows that particles that collect on the fluid surface due to flotation have a larger portion of particles with a diameter of more than 30 µm than the inflow suspension.

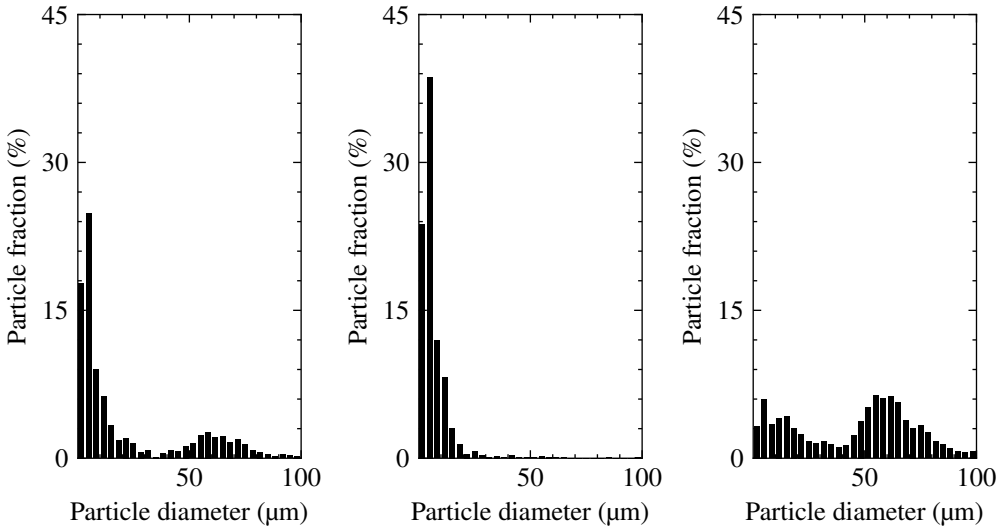

(**a**) Inflow (**b**) Effluent after 20 min (**c**) Particles on fluid surface

Figure 5. PSD of the inflow and outflow suspension and of the particles at the fluid surface for the experiment with 15 ppi, Q = 0.4 L min^{-1} and P = 30%.

In order to further investigate this observation, the quantity ε is derived,

$$\varepsilon = \frac{N_{d<30\,\mu m}}{N_{total}} \cdot 100\% \tag{5}$$

which defines the percentage of particles with a diameter <30 µm in the total number of particles detected in the effluent from the beginning to the end of the experiments. The determined values of ε can be found in Table 3.

Table 3. Overview of all values of ε.

Q	**0.4 L min^{-1}**			**0.8 L min^{-1}**		
Φ	**15 ppi**	**20 ppi**	**30 ppi**	**15 ppi**	**20 ppi**	**30 ppi**
P = 30%	98%	96%	99%	97%	95%	92%
P = 10%	96%	97%	90%	83%	83%	79%
P = 0%	95%	89%	97%	95%	87%	89%

The data show that, for a power output of 30%, more particles with a diameter <30 µm can be detected in the effluent than from smaller power outputs. It is noticeable that ε does not always increase with a higher power input. For all measurements with a flow rate of 0.8 L min^{-1} and a fixed porosity, ε is the smallest for a power output of 10%. The same can be observed for the measurements with a Φ = 30 ppi and Q = 0.4 L min^{-1}. Generally, the portion of small particles is larger for the measurements with Q = 0.4 L min^{-1}, compared to Q = 0.8 L min^{-1}.

4. Discussion

4.1. Flotation

The sound-aided flotation can be explained when looking at the effects that stabilize the suspension in the first place. In general, a differentiation can be made between electrostatic and steric stabilization. Electrostatic stabilization is based on the formation of an electrical double layer on the particle surface, which leads to electrostatic repulsion between the particles. Steric stabilization, on the other hand, results from the absorption of polymer chains on the particle surface, whose interaction with absorbed polymer chains from other particles leads to repulsion. Thus, both stabilization mechanisms depend on the surface area of the particles. The suspension is in a stable state, when these effects can counteract the sedimentation or flotation arising from the density difference between the liquid and solid phase. In the inlet suspension, the stabilization mechanisms and the density-dependent forces are in equilibrium. When the particles interact with the sound field, they begin to agglomerate due to the attractive interaction caused by the SAF. Since SAF scales with particle volume, larger particles are more likely to form agglomerates. This results in a shift of the equilibrium between the particle surface and volume to the detriment of the stabilization mechanisms. Thereby, flotation is enhanced and the particles can be separated from the liquid phase.

4.2. Influence of the Parameters on the Filter Efficiency

Before looking in more detail at the influence of the various parameters on the filter efficiency, it should be pointed out once again that the measured filter efficiency results from the actual filtration and the flotation.

The positive effect a reduction in the flow rate has on the efficiency is rather apparent. With lower velocities, the time that particles remain in the sound field and filter medium increases, giving the particles a higher chance to agglomerate and be retained by the filter. Furthermore, the influence of drag forces decreases, which has the potential to release particles from the filter again.

The fact that changes in porosity did not result in statistically significant changes in the filter efficiencies can be attributed to the experimental setup where the pore size of all the filter media is one magnitude larger than the average particle size. Also, a large portion of the agglomerates that formed in the sound field was larger than the pore size of any of the filter materials. With a smaller ratio of pore size to particle size, a rise in the influence of variation in pore size on filter efficiency is expected.

The increase in filter efficiency due to higher acoustic power can be explained by a characteristic of the PAF and SAF. Both behave proportionally to the acoustic energy density of the sound field which, for higher sound power levels, promotes the agglomeration of the particles and the resulting effects.

4.3. Change in PSD

In surface and depth filtration, it is almost always the case that large particles can be separated more easily than small ones. However, in the experiments performed, the change in PSD under the influence of acoustic forces is significant. Moreover, it is of interest as to especially why the particles with diameters >30 µm are found in the floating particles. A possible explanation is the dependency of PAF and the SAF on particle volume. As a result, particularly large particles are pushed into the wave nodes or antinodes by the PAF, which promotes their agglomeration by the SAF. Thus, the agglomerates are increasingly composed of larger particles, and the surfaced agglomerates have a high fraction of particles with diameters >30 µm.

5. Conclusions

By using a comparatively large channel, it was shown that sound-assisted filtration can be scaled-up from microfluidic applications, and can be used in larger channels, enabling its use for industrial applications. It has been shown that the PAF and SAF promote the separation of the solid and liquid phases of a suspension. This separation is based on the formation of agglomerates, which can be well retained by filter media more easily. The flotation of agglomerates also contributes to the separation of particles from the liquid. The two mechanisms can significantly increase the filter efficiency compared to experiments without a sound field. It is of further interest as to whether sound-assisted flotation can be instrumentalized, and if the filter medium can be replaced by a skimming processes.

Author Contributions: Conceptualization, J.H. and R.S.; methodology J.H.; validation J.H. and R.S.; resources R.S.; data curation J.H.; writing J.H. and R.S.; supervision R.S.; project administration R.S. All authors have read and agreed to the published version of the manuscript.

Funding: This research received no external funding.

Data Availability Statement: Data available in a publicly accessible repository. The data presented in this study are openly available in Zenodo at https://doi.org/10.5281/zenodo.8347908.

Conflicts of Interest: The authors declare no conflict of interest.

Abbreviations

The following abbreviations are used in this manuscript:

ANOVA	Analysis of variance
DoE	Design of experiments
PA	Polyamid 12
PAF	Primary acoustic force
ppi	Pores per inch
PSD	Particle size distribution
SAF	Secondary acoustic force

References

1. Iyare, P.U.; Ouki, S.K.; Bond, T. Microplastics removal in wastewater treatment plants: A critical review. *Environ. Sci. Water Res. Technol.* **2020**, *6*, 2664–2675. [CrossRef]
2. Galgani, F.; Fleet, D.; Van Franeker, J.; Katsanevakis, S.; Maes, T.; Mouat, J.; Oosterbaan, L.; Poitou, I.; Hanke, G.; Thompson, R.; et al. *Marine Strategy Framework Directiv—Task Group 10 Report: Marine Litter*; Publications Office of the European Union: Luxembourg, 2010. [CrossRef]
3. Ajith, N.; Arumugam, S.; Parthasarathy, S.; Manupoori, S.; Janakiraman, S. Global distribution of microplastics and its impact on marine environment—A review. *Environ. Sci. Pollut. Res.* **2020**, *27*, 25970–25986. [CrossRef] [PubMed]
4. Kleinhenz, S. Filtermaterialien für die FVK-Nasszerspanung/Filter materials for FRP machining—Retention rate for filter materials during the wet machining of fiber-reinforced plastics. *Werkstattstech. Online* **2021**, *111*, 343–348. [CrossRef]
5. van der Bruggen, B.; Lejon, L.; Vandecasteele, C. Reuse, treatment, and discharge of the concentrate of pressure-driven membrane processes. *Environ. Sci. Technol.* **2003**, *37*, 3733–3738. [CrossRef]
6. Zhang, S.; Wang, Y.; Onck, P.; den Toonder, J. A concise review of microfluidic particle manipulation methods. *Microfluid. Nanofluidics* **2020**, *24*, 24. [CrossRef]

7. Laurell, T.; Petersson, F.; Nilsson, A. Chip integrated strategies for acoustic separation and manipulation of cells and particles. *Chem. Soc. Rev.* **2007**, *36*, 492–506. [CrossRef] [PubMed]
8. Bruus, H. Acoustofluidics 7: The acoustic radiation force on small particles. *Lab Chip* **2012**, *12*, 1014–1021. [CrossRef] [PubMed]
9. Apfel, R.E. Acoustically induced square law forces and some speculations about gravitation. *Am. J. Phys.* **1988**, *56*, 726–729. [CrossRef]
10. Gupta, S.; Feke, D.L. Acoustically driven collection of suspended particles within porous media. *Ultrasonics* **1997**, *35*, 131–139. [CrossRef]
11. Gupta, S.; Feke, D.L. Filtration of particulate suspensions in acoustically driven porous media. *AIChE J.* **1998**, *44*, 1005–1014. [CrossRef]
12. Grossner, M.T.; Feke, D.L.; Belovich, J.M. Single-collector experiments and modeling of acoustically aided mesh filtration. *AIChE J.* **2005**, *51*, 1590–1598. [CrossRef]
13. Wang, Z.; Grabenstetter, P.; Feke, D.L.; Belovich, J.M. Retention and viability characteristics of mammalian cells in an acoustically driven polymer mesh. *Biotechnol. Prog.* **2004**, *20*, 384–387. [CrossRef] [PubMed]
14. Vytautas, O.; Vytautas, J.; Ievgeniia, G.; Rimvydas, G.; Algiment, A. Separation of Microparticles from Suspension Utilizing Ultrasonic Standing Waves in a Piezoelectric Cylinder Actuator. *Actuators* **2018**, *7*, 14. [CrossRef]
15. Jinzheng, G.; Hongqiang, J.; Yanling, C.; Yiqian, M.; Xiqin, T.; Yuxin, T.; Fuling, Z.; Shishang, G. High-throughput acoustic separation device with impedance-matched channel. *Microfluid. Nanofluidics* **2023**, *27*, 62. [CrossRef]